Electronic Supplementary Information

Anion Coordination Directed Synthesis Patterns for [Ni_4] Aggregates: Structural Changes for Thiocyanate Coordination and Ligand Arm Hydrolysis

ManishaDas,[a] Radovan Herchel,[b] Zdeněk Trávníček,[b] Valerio Bertolasi,[c] Debashis Ray*[a]

[a]*Department of Chemistry, Indian Institute of Technology, Kharagpur 721 302, India*

[b]*Division of Biologically Active Complexes and Molecular Magnets, Regional Centre of Advanced Technologies and Materials, Faculty of Science, Palacký University in Olomouc, 783 71 Olomouc, Czech Republic*

[c]*Dipartimento di Scienze Chimiche e Farmaceutiche, Centro di Strutturistica Diffrattometrica, University of Ferrara, 44121 Ferrara, Italy*

Scheme S1. Some known topologies of nickel(II) complexes

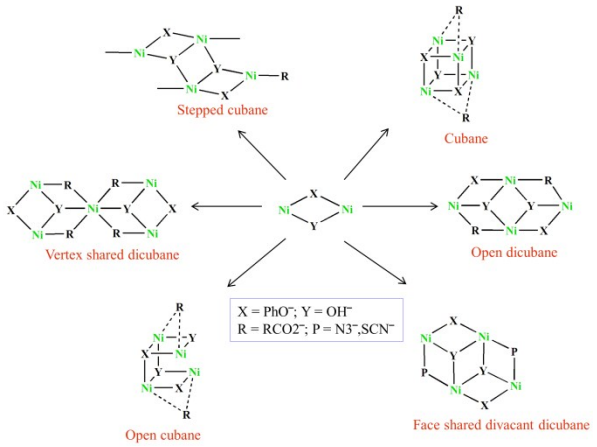

Chart S1. Structural formulas of H_5L1 and H_3L2

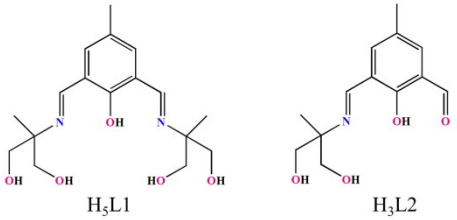

Chart S2. Coordination modes of H_4L1^-, H_2L2^-, HO^-, RCO_2^-, $HAMP^-$ and SCN^-

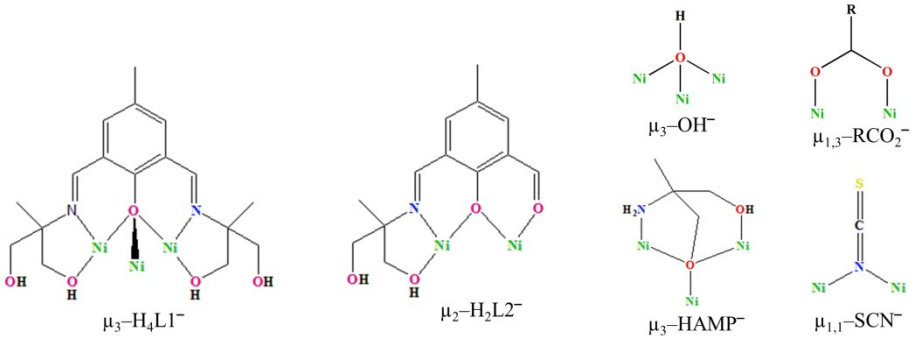

Scheme S2. Synthetic pathway for H_5L1

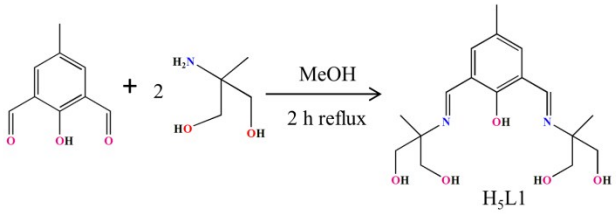

Solid State FTIR Identification

The $\bar{\nu}_{OH}$ stretching vibrations of different origin were observed at 3432, 3460, 3411 and 3402 cm^{-1} for nickel(II) bound alcohol arms of the ligand, bridging –OH groups and lattice water molecules in **1**–**3b** respectively. In many cases the found bands were broad due to extensive H-bonding interactions (Figure S1 in SI). The stretching vibrations from coordinated imine functions ($\bar{\nu}_{C=N}$) of bound Schiff bases were appeared at 1628 cm^{-1} for **1** and **2**, and at 1621cm^{-1} for **3a** and **3b**. Following ligand arm hydrolysis the coordinated $\bar{\nu}_{C=O}$ stretching vibrations were detected at 1637 cm^{-1} for **3a** and **3b**. The presence of carboxylate linkers in **1** and **2** were indicated by the appearance of $\bar{\nu}_{as(COO)}$ at 1570 cm^{-1}, whereas $\bar{\nu}_{s(COO)}$ were found at 1383 and 1384 cm^{-1}. Due to the presence of nitrate as counter anions, peaks at 1383 and 1384 cm^{-1} due to $\bar{\nu}_{s(COO)}$, were broadened as their stretching vibrations also appear in this region. The asymmetric stretching vibration, $\bar{\nu}_{as(COO)}$, of the carboxylate counter anions in **1** and **2** appears at 1645 and 1647 cm^{-1}, whereas the symmetric stretching vibration $\bar{\nu}_{s(COO)}$ appears at 1307 and 1310 cm^{-1} respectively.[R1] The incorporation of the SCN^- groups in place of the OH^- ones were the deciding elements for the generation of partial dicubane aggregates **3a** and **3b** and the very presence of the SCN^- groups were thus established from its characteristic FTIR stretching vibrations. The indicative $\bar{\nu}_{C–N}$ stretching vibrations for **3a** and **3b** appeared as a single intense band at 2020 and 2018 cm^{-1}, respectively.[R2] The $\bar{\nu}_{C–S}$ stretching frequency appears at 753 and 752 cm^{-1} and the N−C−S bending mode (δ_{NCS}) at 440 and 439 cm^{-1}.[R3,R4]

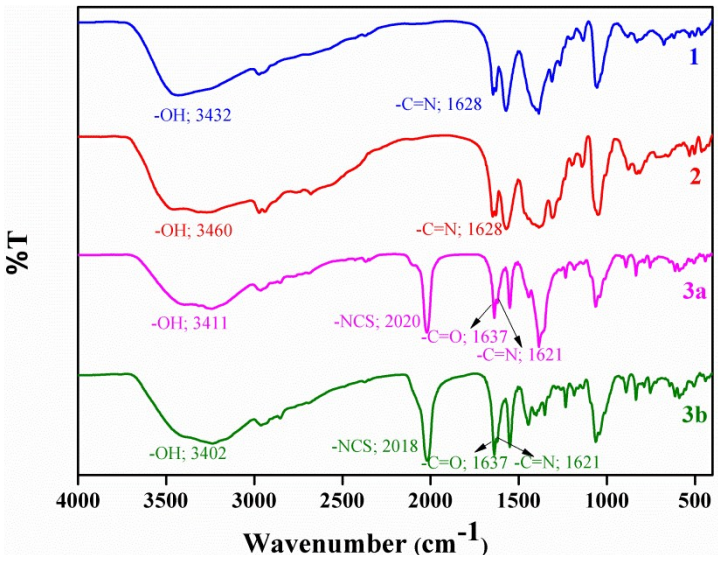

Figure S1. FTIR spectra of **1-3b**.

Powder X-ray Diffraction Patterns

The powder XRD patterns of the bulk materials of the complexes were collected using a Bruker AXS X-ray diffractometer and compared with the simulated one derived from the single crystal X-ray diffraction data. The identical solid state composition of the powder and single-crystalline products for all the four compounds has been monitored and compared for their band positions using FT-IR spectroscopy and powder X-ray diffraction (PXRD) patterns. Figure S2(i) shows that the powder patterns are in good agreement with the simulated ones based on the single crystal X-ray data. The difference in intensity is due to the orientation of the powder samples during experiment. The similarity assumes that the prepared powder samples were phase pure. Profile fitting of the experimental data was also performed utilizing the cell parameters from the single crystal XRD data and the calculated spectra are in well agreement with the experimental one (Figure S2(ii)).

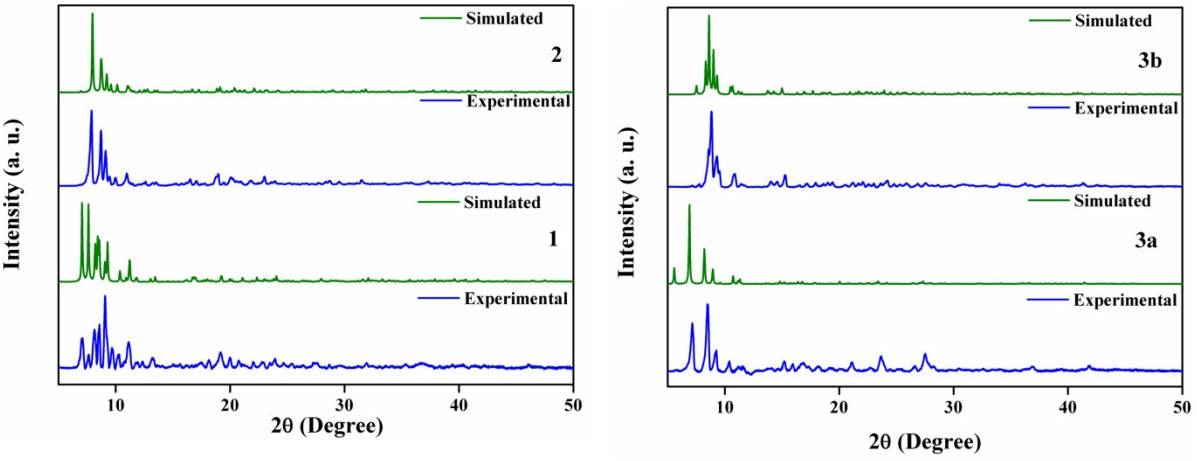

(i)

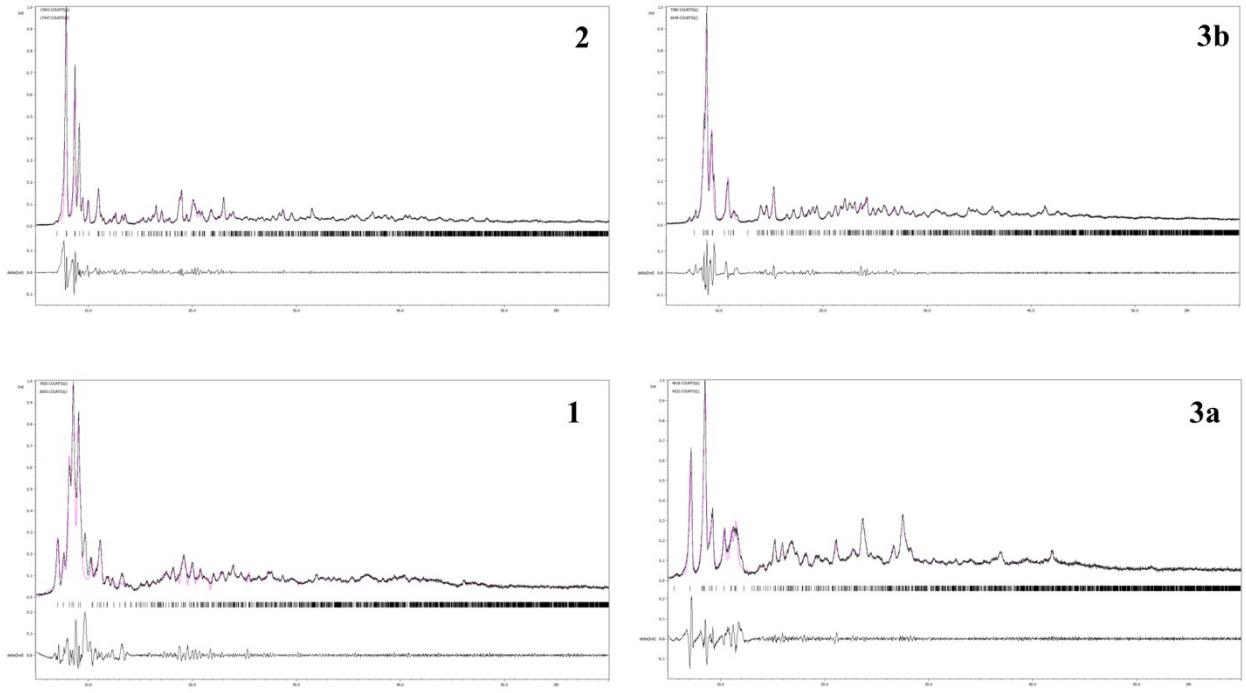

(ii)

Figure S2. Powder XRD pattern (i) and profile fitting of experimental data (ii) of **1**, **2**, **3a** and **3b**.

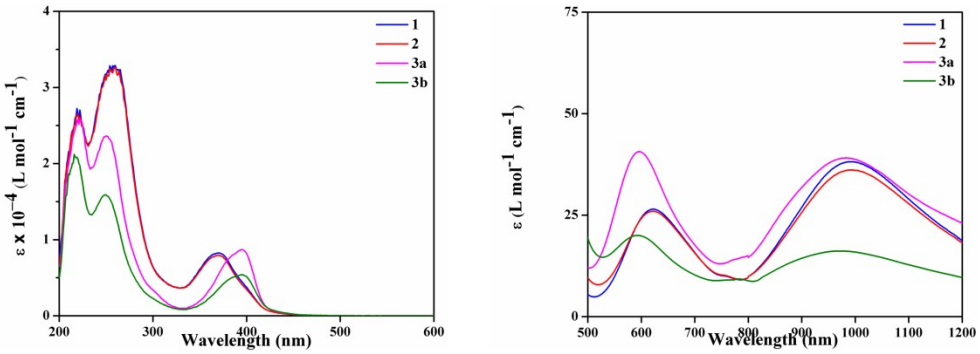

Figure S3. Charge transfer transition (left) and d-d transition (right) of **1**-**3b**.

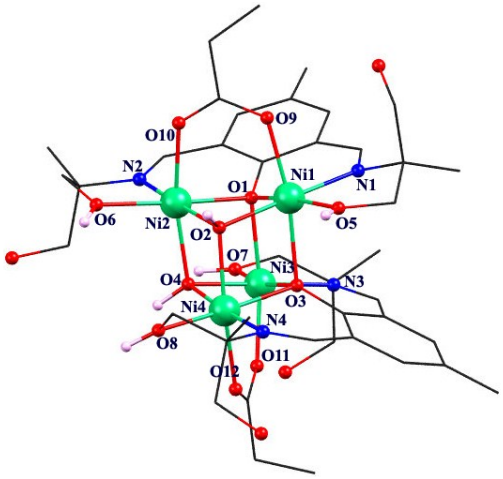

Figure S4. Molecular view of **2** with partial atom numbering scheme. Counter anions are omitted for clarity. H-atoms are shown only for –OH groups. Color code: Ni, green; N, blue; O, red; C, black; H, pink. Ni···Ni distances: Ni1···Ni2, 2.922 Å; Ni3···Ni4, 2.911 Å; Ni1···Ni3, 3.221 Å; Ni1···Ni4, 3.210 Å; Ni2···Ni3, 3.213 Å; Ni2···Ni4, 3.173 Å.

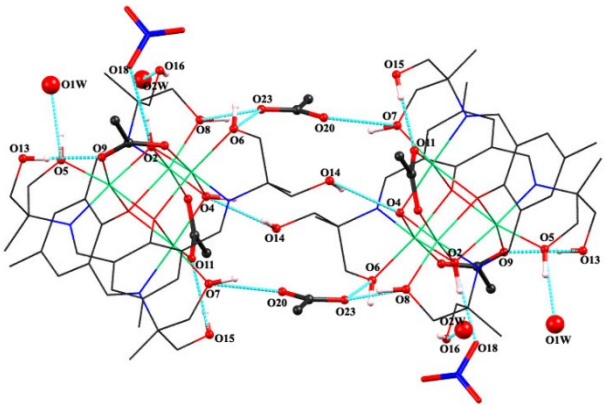

Figure S5. A part of the crystal structure of **1**, showing the extensive network of the O–H···O hydrogen bonds (blue dashed lines).

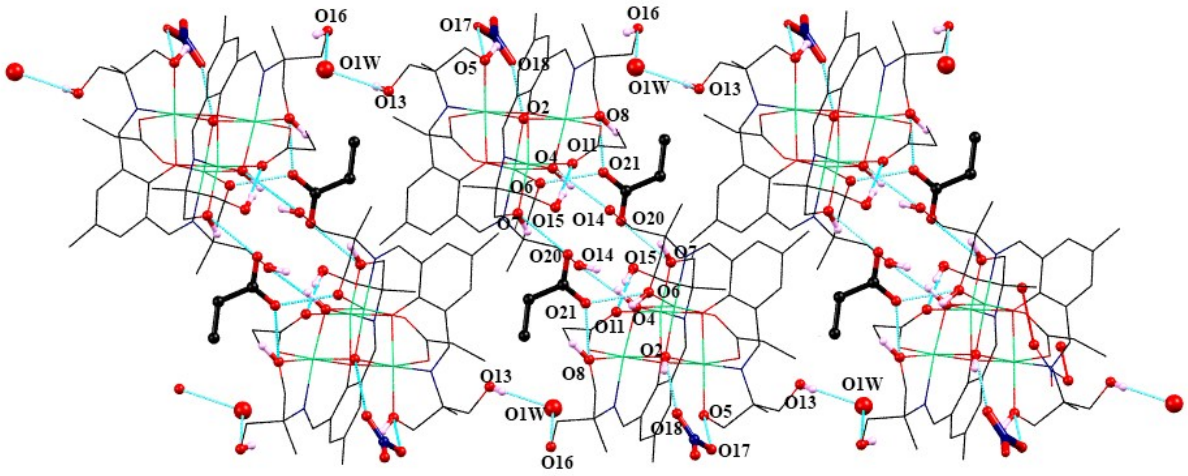

Figure S6. H-bonded double chain formation in **2**.

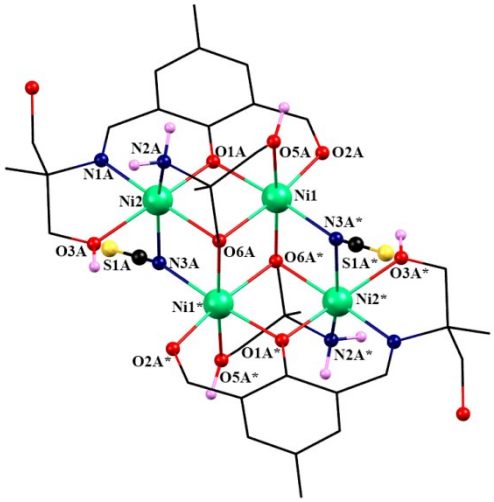

Figure S7. Molecular view of **3b** with partial atom numbering scheme. H-atoms are shown only for –OH and –NH_2 groups. Counter anions are omitted for clarity. Color code: Ni, green; N, blue; O, red; C, black; S, yellow; H, pink.

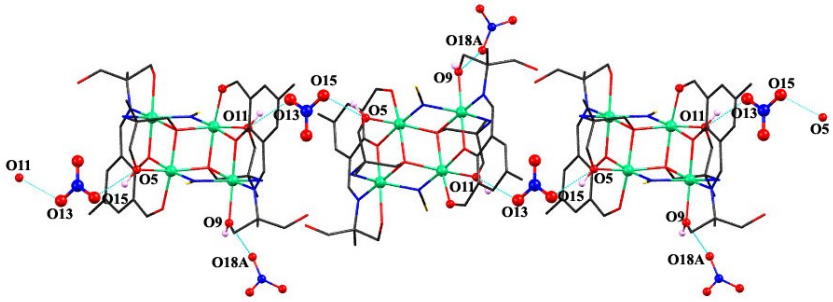

Figure S8. A part of crystal structure of **3a**, showing the O–H···O hydrogen bonds (blue dashed lines) connecting the complex cations and nitrate anions into 1D chain structure.

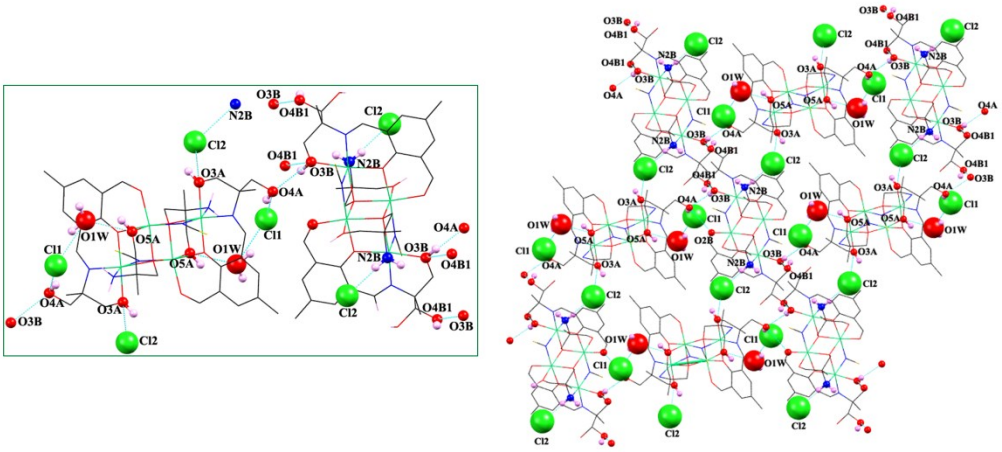

Figure S9. A View of H-bonding interactions (dashed lines) between two tetrameric units (left) and 2D network structure (right) of **3b**.

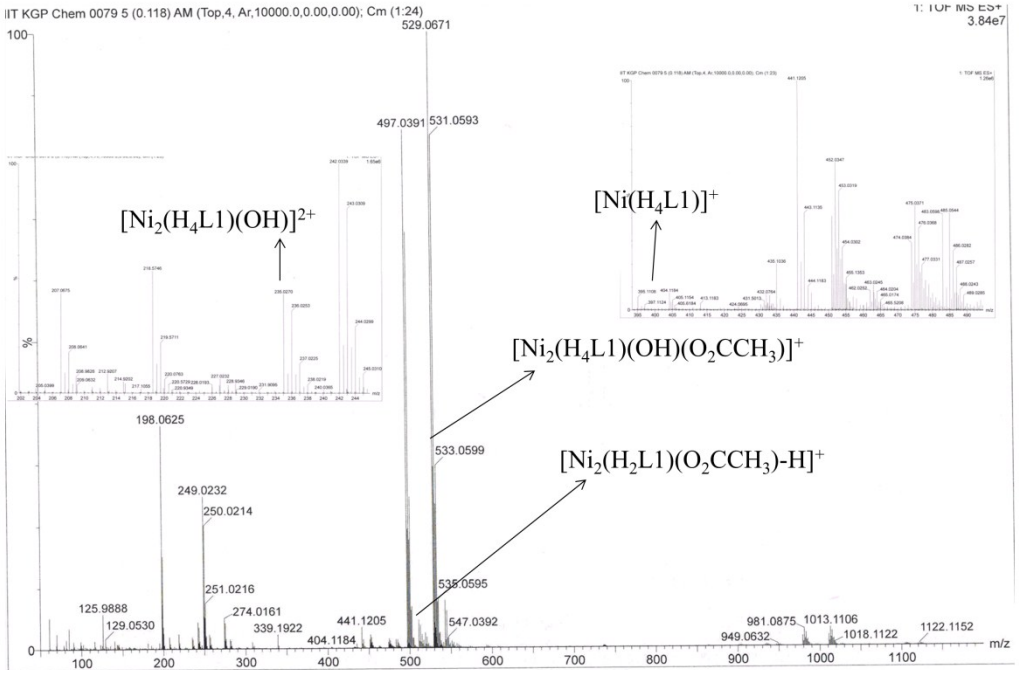

Figure S10. Electrospray mass spectrum (ESI +ve) of **1** in MeOH.

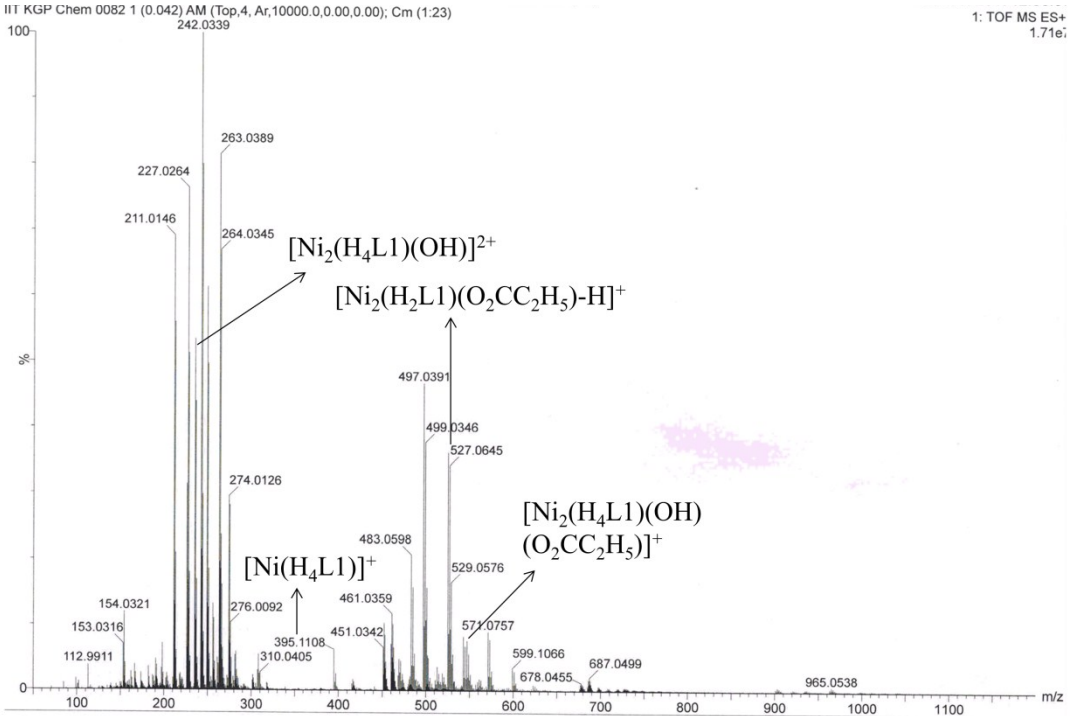

Figure S11. Electrospray mass spectrum (ESI +ve) of **2** in MeOH.

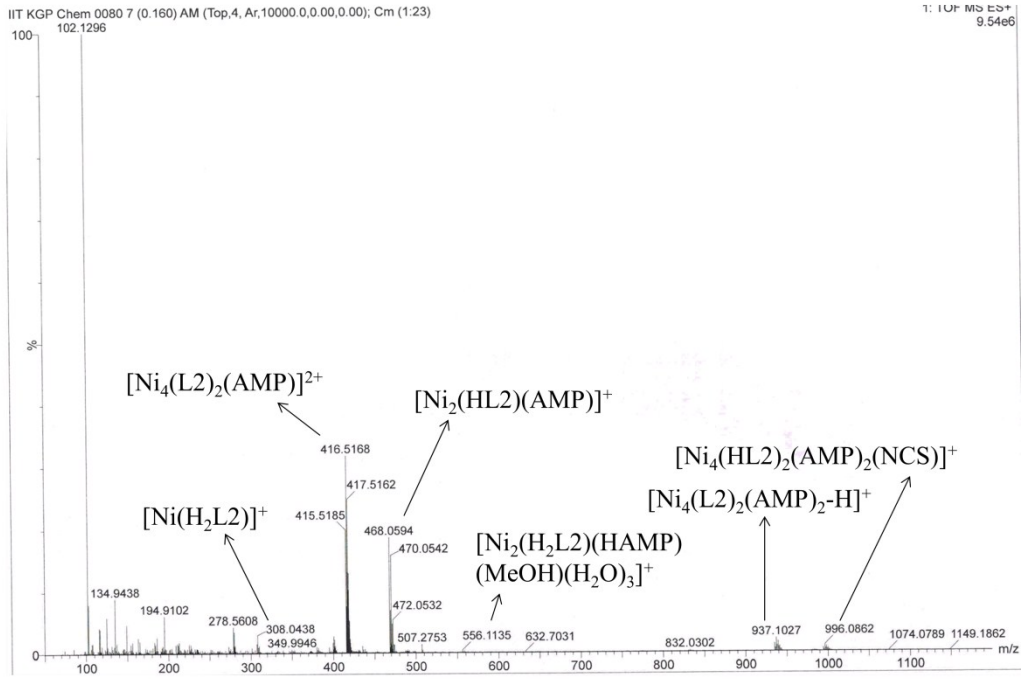

Figure S12. Electrospray mass spectrum (ESI +ve) of **3a** in MeOH.

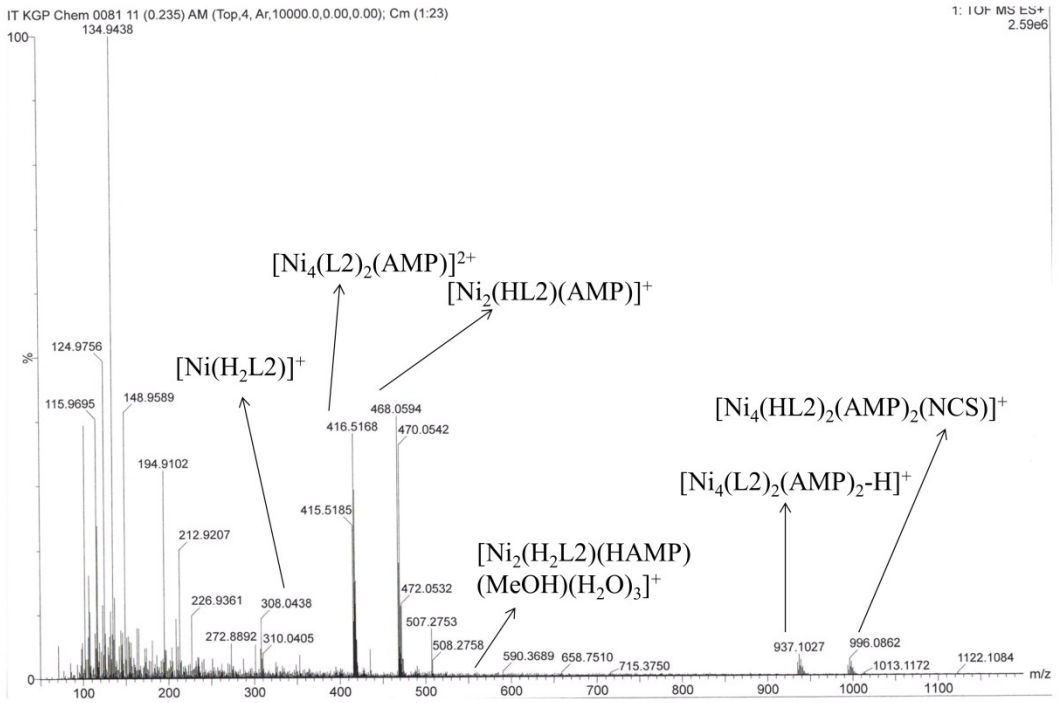

Figure S13. Electrospray mass spectrum (ESI +ve) of **3b** in MeOH.

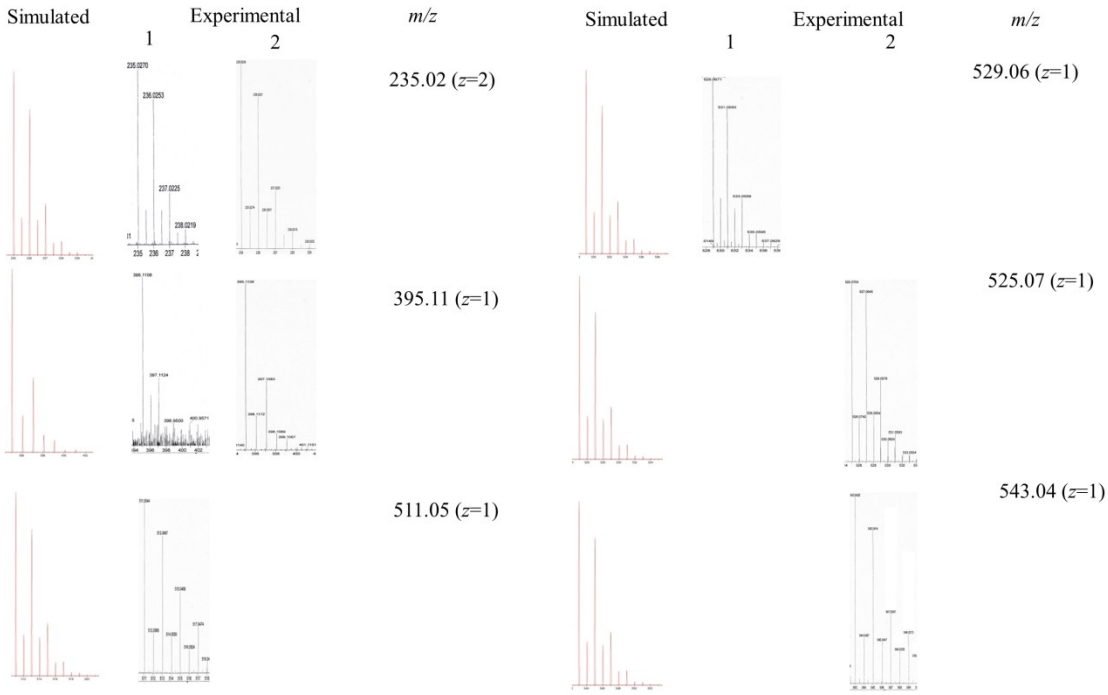

Figure S14. Experimental and simulated isotropic distribution patterns of the peaks of **1** and **2**, respectively, obtained using Electrospray mass spectrum (ESI +ve).

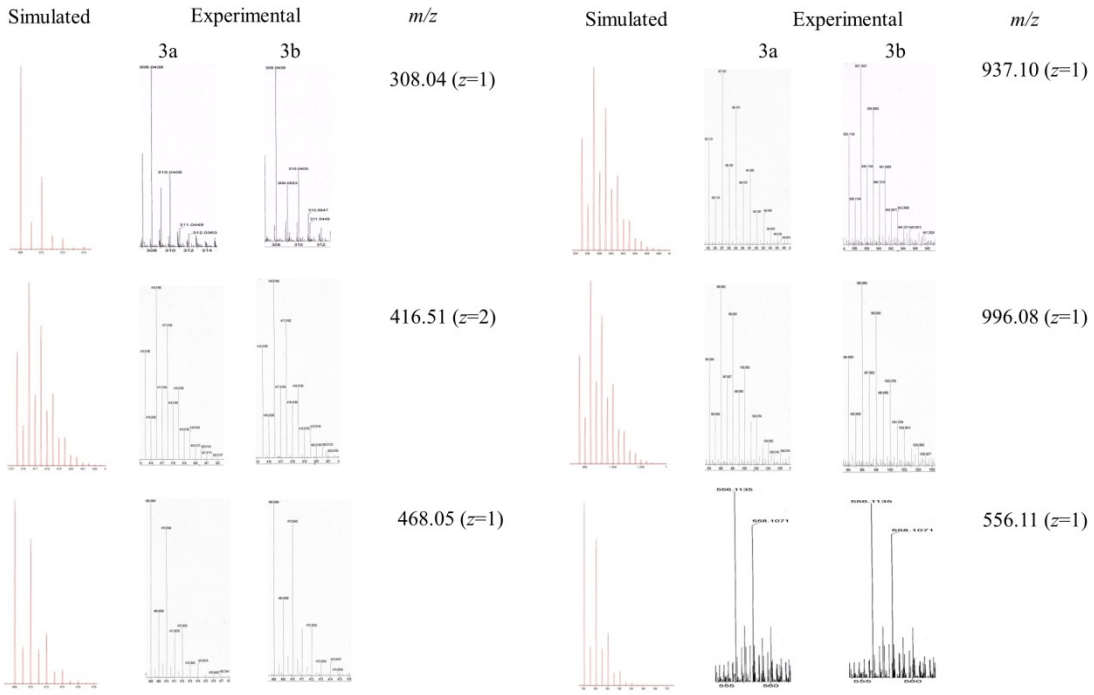

Figure S15. Experimental and simulated isotropic distribution patterns of the peaks of **3a** and **3b**, respectively, obtained using Electrospray mass spectrum (ESI +ve).

EPR Spectra

The X-band EPR spectra recorded on polycrystalline samples of **1-3b** at 298 K is represented in Figure S16. All the complexes showed spectra for a triplet ground spin state (S = 1) as expected for uncoupled Ni^{II} ions. It was possible to simulate the spectra, at least as far as the position of the peaks were concerned to yield the various spin Hamiltonian parameters g_1, g_2 and g_3. However a more rigorous estimation of these parameters and especially D require an EPR spectra at much higher frequencies (HF-EPR).[R5] The parameters obtained are g_1 = 4.40, 4.40, 4.40 and 4.27; g_2 = 2.10, 2.00, 2.00 and 2.10; g_3 = 0.67, 0.67, 0.67 and 0.65; respectively for **1-3b**.

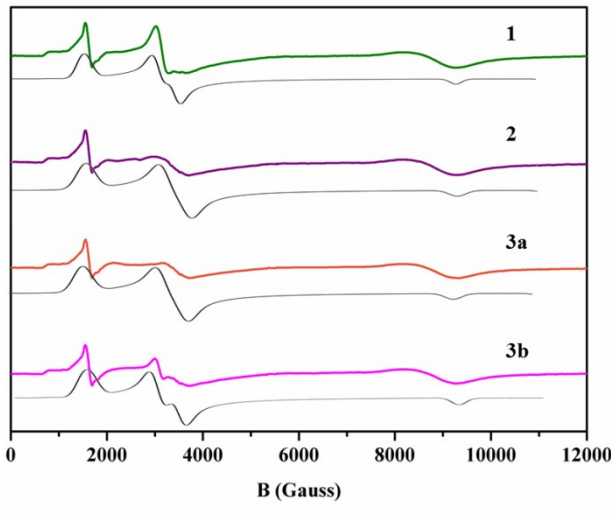

Figure S16. X-band EPR spectra of compounds **1-3b** at 298 K recorded on powdered samples. Green, violet, orange and pink lines represent the experimental spectra. Black lines represent the simulated spectra.

Table S1. Important bond lengths (Å) and angles (°) for **1**, **2**, **3a** and **3b**

Bond lengths (Å)					
Complex **1**					
Ni1–O1	2.051(3)	Ni2–O4	2.075(3)	Ni3–O11	2.043(3)
Ni1–O2	2.017(3)	Ni2–O6	2.072(3)	Ni3–N3	2.004(3)
Ni1–O3	2.184(3)	Ni2–O10	2.083(3)	Ni4–O2	2.066(3)
Ni1–O5	2.052(3)	Ni2–N2	2.011(3)	Ni4–O4	2.034(3)
Ni1–O9	2.045(3)	Ni3–O1	2.193(3)	Ni4–O3	2.083(3)
Ni1–N1	2.000(4)	Ni3–O3	2.053(3)	Ni4–O8	2.059(3)
Ni2–O1	2.071(3)	Ni3–O4	2.014(3)	Ni4–O12	2.051(3)
Ni2–O2	2.031(3)	Ni3–O7	2.056(3)	Ni4–N4	2.009(4)
Ni1–Ni2	2.9229(7)	Ni3–Ni4	2.9061(7)		
Complex **2**					
Ni1–O1	2.0409(19)	Ni2–O4	2.068(2)	Ni3–O11	2.022(2)

Ni1–O2	2.003(2)	Ni2–O6	2.052(2)	Ni3–N3	2.012(3)
Ni1–O3	2.207(2)	Ni2–O10	2.062(2)	Ni4–O2	2.077(2)
Ni1–O5	2.047(2)	Ni2–N2	2.022(2)	Ni4–O3	2.064(2)
Ni1–O9	2.074(2)	Ni3–O1	2.191(2)	Ni4–O4	2.025(2)
Ni1–N1	1.997(3)	Ni3–O3	2.0541(19)	Ni4–O8	2.067(2)
Ni2–O1	2.075(2)	Ni3–O4	2.026(2)	Ni4–O12	2.100(2)
Ni2–O2	2.038(2)	Ni3–O7	2.040(2)	Ni4–N4	2.008(2)
Ni1–Ni2	2.9217(8)	Ni3–Ni4	2.9113(8)		
Complex **3a**					
Ni1–O1	2.023(6)	Ni2–O1	2.001(6)	Ni3–O6	2.056(5)
Ni1–O2	1.998(9)	Ni2–O3	2.104(7)	Ni3–O7	2.025(5)
Ni1–O5	2.067(7)	Ni2–O6	2.033(5)	Ni3–O8	1.988(8)
Ni1–O6	2.049(6)	Ni2–N1	2.012(7)	Ni3–O11	2.080(7)
Ni1–O12	2.058(5)	Ni2–N2	2.100(7)	Ni3–O12	2.047(6)
Ni1–N6	2.127(7)	Ni2–N3	2.191(7)	Ni3–N3	2.115(7)
Ni4–O7	1.996(6)	Ni4–O12	2.011(5)	Ni4–N5	2.093(8)
Ni4–O9	2.105(7)	Ni4–N4	1.995(7)	Ni4–N6	2.208(7)
Complex **3b**					
Ni1–O1A	2.027(3)	Ni2–O6A	2.014(2)	Ni3–O6B*	2.062(3)
Ni1–O2A	2.012(4)	Ni2–N1A	2.001(3)	Ni3–N3B	2.140(4)
Ni1–O5A	2.067(3)	Ni2–N2A	2.105(3)	Ni4–O1B	1.999(3)
Ni1–O6A	2.056(2)	Ni2–N3A	2.268(4)	Ni4–O3B	2.120(3)
Ni1–O6A*	2.059(2)	Ni3–O1B	2.023(3)	Ni4–O6B	2.032(3)
Ni1–N3A	2.114(3)	Ni3–O2B	1.997(4)	Ni4–N1B	1.998(3)
Ni2–O1A	1.995(3)	Ni3–O5B	2.042(4)	Ni4–N2B	2.095(5)
Ni2–O3A	2.094(3)	Ni3–O6B	2.056(3)	Ni4–N3B	2.198(4)

Bond angles (°)					
Complex **1**					
O1–Ni1–O3	80.35(10)	O5–Ni1–O3	92.72(12)	N2–Ni2–O6	81.96(12)
O1–Ni1–O5	168.87(12)	O6–Ni2–O1	171.76(11)	N2–Ni2–O10	91.80(12)
O2–Ni1–O1	86.12(11)	O6–Ni2–O4	101.07(11)	N3–Ni3–O1	101.07(12)
O2–Ni1–O3	79.29(11)	O8–Ni4–O2	97.71(12)	N3–Ni3–O3	90.70(13)
O2–Ni1–O5	101.24(12)	O8–Ni4–O12	90.53(12)	N3–Ni3–O4	177.86(13)
O2–Ni1–O9	92.02(11)	O7–Ni3–O1	90.22(10)	N3–Ni3–O7	81.42(13)
O2–Ni2–O1	85.21(11)	O7–Ni3–O3	166.15(11)	N3–Ni3–O11	87.62(12)
O2–Ni2–O4	78.28(11)	O9–Ni1–O1	93.60(11)	N4–Ni4–O2	97.23(13)
O2–Ni2–O6	103.03(11)	O9–Ni1–O3	169.67(11)	N4–Ni4–O3	89.29(13)
O2–Ni2–O10	90.13(11)	O9–Ni1–O5	94.46(12)	N4–Ni4–O4	173.94(13)
O2–Ni4–O12	169.05(11)	O10–Ni2–O1	93.54(11)	N4–Ni4–O8	80.59(14)
O3–Ni3–O1	80.08(10)	O10–Ni2–O4	167.29(11)	N4–Ni4–O12	91.20(13)
O3–Ni4–O2	80.56(11)	O10–Ni2–O6	86.52(11)	Ni1–O1–Ni2	90.31(10)
O3–Ni4–O8	169.47(11)	O11–Ni3–O1	168.61(11)	Ni1–O1–Ni3	99.66(11
O3–Ni4–O12	92.61(11)	O11–Ni3–O3	92.58(11)	Ni1–O2–Ni2	92.45(11)
O4–Ni2–O1	80.42(10)	O11–Ni3–O7	98.42(11)	Ni1–O2–Ni4	103.01(13)
O4–Ni3–O1	78.90(10)	N1–Ni1–O1	90.60(12)	Ni2–O1–Ni3	97.34(10)
O4–Ni3–O3	87.19(11)	N1–Ni1–O2	176.64(13)	Ni2–O2–Ni4	101.68(12)
O4–Ni3–O7	100.72(11)	N1–Ni1–O3	99.48(13)	Ni3–O3–Ni1	99.91(11)
O4–Ni3–O11	92.14(11)	N1–Ni1–O5	81.90(14)	Ni3–O3–Ni4	89.27(11)
O4–Ni4–O2	78.41(11)	N1–Ni1–O9	88.88(13)	Ni3–O4–Ni2	103.18(12)
O4–Ni4–O3	85.85(11)	N2–Ni2–O1	89.80(12)	Ni3–O4–Ni4	91.78(11)
O4–Ni4–O8	104.06(11)	N2–Ni2–O2	174.75(12)	Ni4–O3–Ni1	96.97(11)
O4–Ni4–O12	92.63(11)	N2–Ni2–O4	99.31(12)	Ni4–O4–Ni2	101.30(12)
Complex **2**					

O1–Ni1–O3	81.36(8)	O2–Ni1–O3	78.54(8)	N1–Ni1–O3	99.64(9)
O1–Ni1–O5	168.29(9)	O2–Ni1–O9	93.27(9)	N1–Ni1–O5	82.51(10)
O1–Ni1–O9	91.67(8)	O5–Ni1–O3	90.12(9)	N1–Ni1–O1	90.96(9)
O2–Ni1–O1	86.52(8)	O5–Ni1–O9	97.82(9)	N1–Ni1–O2	177.08(9)
O2–Ni1–O5	99.71(9)	O9–Ni1–O3	169.49(8)	N1–Ni1–O9	88.27(10)
O2–Ni2–O1	84.72(8)	O7–Ni3–O3	167.36(9)	O8–Ni4–O2	94.80(9)
O2–Ni2–O4	78.45(8)	O7–Ni3–O1	90.60(8)	O8–Ni4–O12	95.57(9)
O2–Ni2–O6	103.40(9)	O11–Ni3–O1	168.86(8)	N4–Ni4–O2	97.86(9)
O2–Ni2–O10	90.94(8)	O11–Ni3–O3	94.82(8)	N4–Ni4–O3	91.33(9)
O4–Ni2–O1	80.31(8)	O11–Ni3–O7	94.73(9)	N4–Ni4–O4	175.90(9)
O6–Ni2–O1	171.86(8)	N3–Ni3–O1	101.45(9)	N4–Ni4–O8	79.83(10)
O6–Ni2–O4	100.66(9)	N3–Ni3–O3	90.13(9)	N4–Ni4–O12	90.77(9)
O6–Ni2–O10	87.44(9)	N3–Ni3–O7	81.77(9)	Ni1–O1–Ni2	90.45(8)
O10–Ni2–O1	92.96(9)	O11–Ni3–O4	90.82(9)	Ni1–O1–Ni3	99.05(8)
O10–Ni2–O4	167.85(8)	N3–Ni3–O4	176.54(8)	Ni2–O1–Ni3	97.70(8)
N2–Ni2–O2	174.36(9)	N3–Ni3–O11	89.01(9)	Ni1–O2–Ni2	92.61(9)
N2–Ni2–O6	82.08(9)	O3–Ni4–O2	80.26(8)	Ni1–O2–Ni4	103.76(10)
N2–Ni2–O10	90.67(9)	O3–Ni4–O12	90.61(9)	Ni2–O2–Ni4	100.89(9)
N2–Ni2–O4	99.35(9)	O2–Ni4–O12	167.53(8)	Ni3–O3–Ni4	89.96(8)
N2–Ni2–O1	89.79(9)	O3–Ni4–O8	169.25(8)	Ni3–O3–Ni1	98.12(8)
O3–Ni3–O1	81.46(8)	O4–Ni4–O2	78.51(8)	Ni4–O3–Ni1	97.39(8)
O4–Ni3–O1	78.51(8)	O4–Ni4–O8	102.28(9)	Ni3–O4–Ni4	91.88(8)
O4–Ni3–O3	86.44(8)	O4–Ni4–O12	92.52(8)	Ni3–O4–Ni2	103.38(9)
O4–Ni3–O7	101.68(8)	O4–Ni4–O3	86.18(8)	Ni4–O4–Ni2	101.63(8)
Complex **3a**					
O1–Ni1–O6	81.3(2)	O3–Ni2–N3	87.1(3)	O6–Ni3–N3	83.8(2)
O1–Ni1–O12	96.7(2)	O6–Ni2–N2	81.8(3)	O7–Ni3–N3	173.9(3)
O2–Ni1–O1	88.7(3)	O1–Ni2–N3	90.5(3)	O8–Ni3–N3	96.9(3)

O2–Ni1–O5	91.4(4)	O6–Ni2–N3	82.4(2)	O11–Ni3–N3	88.2(3)
O2–Ni1–O6	170.0(3)	O1–Ni2–N1	92.2(3)	O12–Ni3–N3	93.5(3)
O2–Ni1–O12	97.9(3)	N1–Ni2–O3	80.8(3)	O7–Ni4–O9	172.8(2)
O1–Ni1–O5	90.5(3)	N1–Ni2–O6	172.5(2)	O7–Ni4–O12	82.0(2)
O6–Ni1–O5	90.2(3)	N1–Ni2–N2	103.8(3)	O12–Ni4–O9	103.6(2)
O6–Ni1–O12	81.9(2)	N1–Ni2–N3	92.6(3)	O7–Ni4–N5	93.5(3)
O12–Ni1–O5	168.3(3)	N2–Ni2–N3	162.5(3)	O7–Ni4–N6	90.0(3)
O1–Ni1–N6	174.3(3)	O7–Ni3–O6	96.5(2)	O12–Ni4–N5	82.7(3)
O2–Ni1–N6	96.9(3)	O7–Ni3–O11	90.6(3)	O12–Ni4–N6	82.8(2)
O5–Ni1–N6	88.2(3)	O7–Ni3–O12	80.4(2)	O9–Ni4–N6	86.3(3)
O6–Ni1–N6	93.1(3)	O8–Ni3–O6	98.1(3)	N4–Ni4–O7	92.4(3)
O12–Ni1–N6	83.7(2)	O8–Ni3–O7	89.1(3)	N4–Ni4–O9	81.5(3)
O1–Ni2–O3	172.5(2)	O8–Ni3–O12	169.5(3)	N4–Ni4–O12	172.6(3)
O1–Ni2–O6	82.3(2)	O8–Ni3–O11	91.0(3)	N5–Ni4–O9	91.7(3)
O6–Ni2–O3	104.4(2)	O6–Ni3–O11	168.6(3)	N4–Ni4–N5	102.6(3)
O1–Ni2–N2	94.8(3)	O12–Ni3–O6	82.0(2)	N4–Ni4–N6	92.4(3)
O3–Ni2–N2	89.5(3)	O12–Ni3–O11	90.4(3)	N5–Ni4–N6	164.4(3)
Ni2–O1–Ni1	99.0(2)	Ni3–O12–Ni1	98.1(2)	Ni4–O7–Ni3	99.3(2)
Ni2–O6–Ni1	97.1(2)	Ni4–O12–Ni1	100.6(2)	Ni1–N6–Ni4	92.5(3)
Ni1–O6–Ni3	98.1(2)	Ni4–O12–Ni3	98.0(2)		
Ni2–O6–Ni3	100.1(2)	Ni3–N3–Ni2	93.4(3)		
Complex **3b**					
O1A–Ni1–N3A	171.71(12)	O2B–Ni3–O6B	169.34(14)	O6B–Ni4–N3B	82.41(13)
O1A–Ni1–O5A	85.65(13)	O2B–Ni3–O6B*	95.37(15)	N1A–Ni2–O3A	82.30(14)
O1A–Ni1–O6A	80.90(10)	O2B–Ni3–N3B	95.24(16)	N1A–Ni2–O6A	172.67(12)
O1A–Ni1–O6A*	96.60(10)	O3A–Ni2–N2A	91.07(14)	N1A–Ni2–N2A	102.98(14)
O1A–Ni2–O3A	169.45(13)	O3A–Ni2–N3A	82.49(14)	N1A–Ni2–N3A	92.69(13)

O1A–Ni2–O6A	82.72(10)	O3B–Ni4–N3B	88.83(15)	N1B–Ni4–O1B	91.54(12)
O1A–Ni2–N1A	91.59(13)	O5A–Ni1–N3A	91.18(14)	N1B–Ni4–O3B	79.96(13)
O1A–Ni2–N2A	98.70(13)	O5B–Ni3–O6B	90.70(16)	N1B–Ni4–O6B	172.76(12)
O1A–Ni2–N3A	89.25(12)	O5B–Ni3–O6B*	170.79(15)	N1B–Ni4–N2B	102.2(2)
O1B–Ni3–O5B	88.48(16)	O5B–Ni3–N3B	91.49(17)	N1B–Ni4–N3B	94.36(14)
O1B–Ni3–O6B	80.74(11)	O6A–Ni1–N3A	91.53(12)	N2A–Ni2–N3A	162.14(14)
O1B–Ni3–O6B*	96.09(12)	O6A*–Ni1–N3A	85.54(12)	N2B–Ni4–O3B	86.13(18)
O1B–Ni3–N3B	175.51(13)	O6A–Ni1–O5A	91.26(12)	N2B–Ni4–N3B	161.5(2)
O1B–Ni4–O3B	171.41(12)	O6A*–Ni1–O5A	172.00(12)	Ni1–O6A–Ni1	98.45(10)
O1B–Ni4–N2B	96.95(18)	O6A–Ni1–O6A	81.55(10)	Ni1–N3A–Ni2	90.91(13)
O1B–Ni4–N3B	90.62(14)	O6A–Ni2–O3A	102.60(11)	Ni2–O1A–Ni1	98.86(11)
O2A–Ni1–O1A	88.86(13)	O6A–Ni2–N2A	82.52(12)	Ni2–O6A–Ni1	97.32(10)
O2A–Ni1–N3A	98.93(15)	O6A–Ni2–N3A	82.67(11)	Ni2–O6A*–Ni1	100.19(10)
O2A–Ni1–O5A	92.32(15)	O6B–Ni3–O6B	82.19(13)	Ni3–O6B–Ni3	97.81(13)
O2A–Ni1–O6A	168.86(13)	O6B*–Ni3–N3B	83.32(13)	Ni3–N3B–Ni4	93.19(15)
O2A–Ni1–O6A*	95.40(13)	O6B–Ni3–N3B	94.78(13)	Ni4–O1B–Ni3	99.60(11)
O2B–Ni3–O1B	89.24(14)	O6B–Ni4–O3B	106.36(12)	Ni4–O6B–Ni3	97.23(11)
O2B–Ni3–O5B	92.67(19)	O6B–Ni4–N2B	82.0(2)	Ni4–O6B*–Ni3	100.92(12)

Table S2. Hydrogen bonding parameters for **1-3b**

Interactions	Type of H-bond	D–H (Å)	D···A (Å)	H···A (Å)	D–H···A (Å)
Complex **1**					
O2–H2···O18		0.98	2.938(6)	1.98	166
O4–H4···O14		0.98	2.947(4)	2.08	147
O5–H5···O1W		0.93	2.647(5)	1.94	131
O6–H6···O23		0.93	2.564(5)	1.97	120
O7–H7···O20		0.93	2.601(4)	1.88	133

O8–H8···O23		0.93	2.648(5)	2.14	113
O13–H13···O9	Intra	0.82	2.705(5)	1.90	166
O14–H14···O4		0.82	2.947(4)	2.26	142
O15–H15···O11	Intra	0.82	2.722(5)	1.91	169
O16–H16···O2W		0.82	2.943(9)	2.24	144
Complex **2**					
O2–H2···O18		0.89(3)	2.937(3)	2.08(4)	161(3)
O4–H4···O14		0.82(3)	2.928(3)	2.14(3)	163(3)
O5–H5···O17		0.91(6)	2.653(3)	1.77(6)	164(5)
O6–H6···O21		0.81(4)	2.562(3)	1.76(4)	173(3)
O7–H7···O20		0.81(3)	2.584(3)	1.78(3)	170(5)
O8–H8···O21		0.91(6)	2.616(3)	1.74(6)	161(5)
O13–H13···O1W		0.82	2.776(5)	2.13	135
O14–H14···O20		0.85(4)	2.723(3)	1.88(4)	173(4)
O15A–H15A···O11	Intra	0.82	2.707(4)	1.90	169
O16–H16···O1W		0.97(4)	2.673(5)	1.71(4)	170(4)
O1W–H1WA···O12		0.95(4)	2.861(4)	1.92(4)	174(6)
Complex **3a**					
O5–H5···O15		0.93	2.635(12)	1.80	147
O9–H9···O18A		0.93	2.77(3)	2.11	127
O11–H11···O13		0.93	2.618(13)	1.78	148
Complex **3b**					
O1W–H1W···Cl1		1.01	3.0946	2.17	151
O3A–H3A1···Cl2		0.93	2.9609	2.29	129
O4A–H4A···Cl1		0.91	3.0335	2.17	157
O5A–H5A1···O1W		0.93	2.7456	2.05	131
O3B–H3B1···O4B1		0.93	2.9316	2.20	135

O3B–H3B1···O4A		0.93	2.7622	2.15	122
N2B–H2B1···Cl2		0.89	3.2434	2.36	173

Table S3. Crystal data and structure refinement details for compounds **1**, **2**, **3a** and **3b**

parameters	**1**	**2**	**3a**	**3b**
Formula	$C_{40}H_{65}N_5Ni_4O_{24}$	$C_{45}H_{72}N_6Ni_4O_{22.5}$	$C_{36}H_{52}N_8Ni_4O_{18}S_2$	$C_{37}H_{58}Cl_2N_6Ni_4O_{14}S_2$
F.W. (g mol^{-1})	1234.78	1291.83	1183.74 g mol^{-1}	1180.75 g mol^{-1}
crystal system	Triclinic	Triclinic	Monoclinic	Triclinic
space group	$P\bar{1}$	$P\bar{1}$	$P2_1/n$	$P\bar{1}$
Crystal color	Green	Green	Green	Green
Crystal size/mm^3	0.34×0.26×0.18	0.36×0.25×0.17	0.36×0.25×0.17	0.43×0.19×0.12
a/ Å	11.6627(6)	11.186(3)	12.0157(14)	11.8297(4)
b/ Å	12.5163(6)	12.760(4)	25.622(3)	13.0777(5)
c/ Å	19.6420(9)	19.351(5)	20.278(2)	19.8873(5)
α/ deg	92.6980(10)	95.105(7)	90	89.9710(17)
β/ deg	96.2000(10)	95.350(7)	95.703(5)	74.6770(15)
γ / deg	90.0900(10)	94.242(7)	90	64.9690(12)
V/ Å^3	2847.2(2)	2729.6(13)	6212.0(12)	2666.71(15)
Z	2	2	4	2
D_c/g cm^{-3}	1.437	1.569	1.266	1.470
μ (mm^{-1})	1.381	1.443	1.322	1.630
F(000)	1282	1348	2448	1224.0
T/K	293(2)	293(2)	300(2)	295
Total reflections	34906	33595	46969	31349
R(int)	0.0377	0.0357	0.0498	0.0642
Unique reflections	11167	10741	10793	15385
Observed reflections	9138	9064	7847	11442
Parameters	691	797	631	602
R_1; wR_2 ($I > 2\sigma(I)$)	0.0555, 0.1686	0.0403, 0.1214	0.0915, 0.2931	0.0676, 0.2220
GOF (F^2)	1.077	1.046	1.101	1.059

Largest diff peak and hole (e $Å^{-3}$)	2.552, -1.093	1.985, -0.821	1.611, -1.405	1.294, -0.720
CCDC No.	1835111	1835112	1835113	1835110

$R_1 = \Sigma(||F_o|-|F_c||)/\Sigma|F_o|$. $wR_2 = [\Sigma w(|F_o|-|F_c|)^2/\Sigma w(F_o)^2]^{1/2}$. $w = 0.75/(\sigma^2(F_o) +0.0010F_o^2)$.

References

R1 K. Nakamoto, *Infrared and Raman Spectra of Inorganic and Coordination Compounds*,4th ed.; Wiley: New York, 1986.

R2 R. Cortes, M. K. Urtiaga, L. Lezama, J. L. Pizarro, M. I. Arriortua and T. Rojo, *Inorg. Chem*., 1997, **36**, 5016-5021.

R3 W.-H. Zhang, Y.-L. Song, Z.-G. Ren, H.-X. Li, L.-L. Li, Y. Zhang and J.-P. Lang, *Inorg.Chem*., 2007, **46**, 6647–6660.

R4 R. H. Toeniskoetter and S. Solomon, *Inorg. Chem*., 1968, **7**, 617–620.

R5. S. Petit, P. Neugebauer, G. Pilet, G. Chastanet, A.-L. Barra, A. B. Antunes, W. Wernsdorfer and D. Luneau, *Inorg. Chem*., 2012, **51**, 6645−6654.